

Diamond-based Biosensors with an Impedimetric and Label-free Read-out

V. Vermeeren^{*}, L. Grieten^{**}, Natalie Vanden Bon^{*}, K. Haenen^{****}, P. Wagner^{**} and L. Michiels^{*}

^{*}Hasselt University, Biomedical Research Institute, Agoralaan Bldg. C and D, B-3590 Diepenbeek, Belgium

^{**}Hasselt University, Institute for Materials Research, Wetenschapspark 1, B-3590 Diepenbeek, Belgium

^{****}Division IMOMEC, IMEC vzw, Wetenschapspark 1, B-3590 Diepenbeek, Belgium

ABSTRACT

Healthcare and diagnostics is slowly moving towards molecular medicine and point-of-care diagnosis. Electronic biosensors can offer opportunities in this area that the current state-of-the-art, such as denaturing gradient gel electrophoresis (DGGE) for mutation analysis and ELISA for abnormal protein detection, is unable to fulfill. We developed an electronic DNA- and immunosensor based on nanocrystalline diamond (NCD) and electrochemical impedance spectroscopy (EIS). During DNA hybridization and denaturation, a difference is observed for 1-mismatch target DNA and complementary target DNA in real-time. Our immunosensor was made to detect C-Reactive Protein (CRP), a risk marker for cardiovascular diseases. The specificity of the immunosensor was demonstrated by the incubation with CRP and the non-specific plasminogen. Since 10 nM of CRP was still clearly distinguishable from buffer, our prototype reached a sensitivity that is in the clinically relevant concentration ranges.

Keywords: denaturation, DNA-sensor, hybridization, immunosensor, impedance spectroscopy

1 INTRODUCTION

The evolution from ‘micro’-science into ‘nano’-science has blossomed with the dawn of bio-electronics: a scientific field coupling the achievements in molecular biology with the advances in electronics to obtain higher sensitivity, specificity and speed.

Especially healthcare and diagnostics can benefit from this newly developing science, since they are moving more and more towards molecular medicine. Hence, a lot of research is being performed on biosensors, which have played a pivotal role in this research field. Biosensors are analytical devices consisting of biomolecules serving as recognition elements, coupled to a solid physical transducer. This transducer ‘translates’ the biological recognition event between the receptor molecule and its target into a readable signal. However, rarely one has made it to point-of-care applications because of the expensive and bulky infrastructure required for signal read-out.

Electronic read-out methods, such as electrochemical impedance spectroscopy (EIS), are preferred for this, since they allow real-time and label-free signal generation and cheap implementation, because of the well-understood silicon (Si) microprocessing techniques.

However, it is known that the covalent bond between Si and biomolecules is fairly weak, causing the gradual loss of bioreceptors from the surface, and hence a drift in signal

and decrease in sensitivity and reliability [1]. Diamond is an attractive alternative, because of its semiconductive nature by doping, its chemical inertness, and its ability to be biofunctionalized [1,2]. Furthermore, diamond, being a carbon (C) lattice, can form stable C-C bonds with biomolecules, creating a very stable interface between transducer and receptor molecules, and hence a stable signal [1].

For these reasons, our goal was to develop prototypes of impedimetric nanocrystalline diamond (NCD)-based biosensors. We focused on the development of DNA- and immunosensors, since the majority of all diagnostic tests involve either mutation analysis or abnormal protein detection, respectively.

2 MATERIALS AND METHODS

2.1 DNA-Sensor

We previously designed a simple, efficient two-step protocol for the covalent attachment of ssDNA to NCD. Briefly, ω -unsaturated fatty acids are photochemically bound to H-terminated NCD, yielding a COOH-terminated NCD surface. NH₂-modified ssDNA, with a sequence corresponding to a fragment of the Phenylalanine Hydroxylase (PAH) gene, is covalently linked to these COOH-groups, using 1-ethyl-3-(3-dimethylaminopropyl)-carbodiimide (EDC) [3,4]. Mutations in this gene cause the disease Phenylketonuria (PKU), an inability to metabolize phenylalanine to tyrosine due to the absence of PAH.

The next step towards the development of a prototype of a label-free DNA-sensor involved the study of the electronic properties of DNA-functionalized NCD using EIS. The interface properties are expected to change differently upon hybridization with complementary versus non-complementary DNA. The impedance spectra were obtained in a frequency range between 100 Hz and 1 MHz.

2.2 Immunosensor

We also developed a prototype of a label-free NCD-based impedimetric immunosensor by adsorption of anti-C-Reactive Protein (anti-CRP) onto H-terminated NCD. CRP is an acute phase protein that serves as an important risk assessment factor for the development of cardiovascular diseases [5].

EIS was used to detect the changes in electronic interface properties upon recognition of CRP by anti-CRP. The specificity of the system was tested with the non-specific plasminogen. Sensitivity experiments were also

performed with different concentrations of CRP. The impedance spectra were obtained in a frequency range between 100 Hz and 1 MHz.

2.3 Experimental Setup

NCD samples of 1 cm² coated with either ssDNA or anti-CRP antibodies, functioning as working electrodes, were mounted on a copper (Cu) back contact using silver (Ag) paste. Rubber O-rings with a diameter of 6 mm and an acrylic glass lid containing circular openings of equal size were pressed onto the samples to create reaction wells above the NCD samples. Each well was filled with 140 μ l of reaction fluid. Gold (Au) wires, placed \sim 1 mm above each NCD surface and in contact with the reaction fluid, were used as counter-electrodes [6,7].

EIS was performed using a Hewlett Packard 4194A Impedance/Gain-Phase Analyzer (Agilent, Diegem, Belgium). The impedance is measured by applying an AC potential of 10 mV to the measurement cell. The response to this potential is an AC current signal. The complex impedance was measured for 50 frequencies, equidistant on a logarithmic scale, in a frequency range from 100 Hz to 1 MHz [6,7].

Real-time impedance spectra were collected during DNA hybridization and denaturation, and during CRP recognition. For hybridization, 4 μ M of either complementary or 1-mismatch ssDNA was added to the reaction wells. Subsequently, the DNA strands were denatured by filling the wells with 0.1 M NaOH [6]. For the immunosensor specificity experiments, 500 nM of either CRP or plasminogen was added to the reaction wells. For the sensitivity analysis 100, 10 or 0 nM of CRP was added to the reaction wells.

3 RESULTS AND DISCUSSION

3.1 DNA-Sensor

3.1.1 Hybridization

As shown in Figure 1, complementary and 1-mismatch ssDNA can be impedimetrically differentiated in real-time during hybridization at intermediate frequencies (\sim 1 kHz), even in the first 10 minutes after target DNA addition.

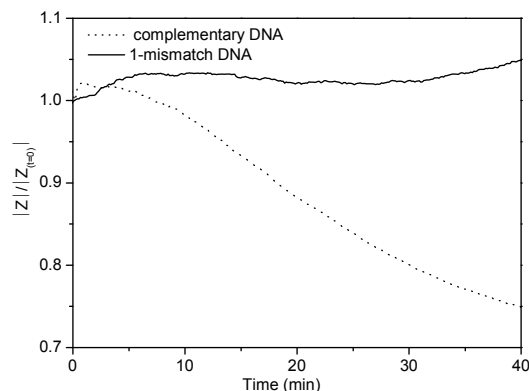


Figure 1: Real-time impedance curves during hybridization with complementary ssDNA (full line) and 1-base mismatch ssDNA (dotted line) at 1150 Hz.

In order to get more insight in the electrical properties of the semiconducting layer during hybridization, the impedance spectra were analyzed using an equivalent circuit model (Figure 2) [1].

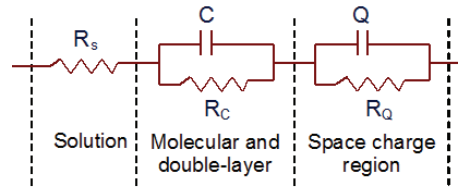


Figure 2: The electrical circuit model used for fitting the impedance data.

It can be divided into three components: (a) the solution resistance, R_s , between the Au electrode and the NCD surface, (b) a resistance R_c and a capacitor C in parallel, attributed to the molecular layer and double-layer, and (c) a resistance R_Q and a constant phase element Q in parallel, corresponding to the space-charge region in the NCD. Table 1 gives the values of the electrical elements after fitting the measured data to the electrical circuit. The observed decrease in R_Q and increase in Q , which was reproducible, can be rationalized in terms of the depletion zone in the space-charge region of a semiconductor. During hybridization, the amount of negative charges near the diamond surface will increase and will attract the positive charge carriers inside the diamond bulk. As a result, the depletion zone will be smaller for samples with dsDNA. This will result in a decrease in the resistance R_Q and possibly in a higher Q value [6].

Element	Before hybridization	After hybridization
R_s (Ω)	222 \pm 14	205 \pm 12
C (nF)	436 \pm 10	369 \pm 6
R_c (k Ω)	26 \pm 6	30 \pm 5
Q (nS.s ⁿ)	14.4 \pm 1.5	13.6 \pm 1.0
n	0.888 \pm 0.009	0.896 \pm 0.008
R_Q (k Ω)	3.49 \pm 0.04	3.02 \pm 0.03

Table 1: Results of fitting the impedance spectra before and after hybridization with complementary DNA.

3.1.2 Denaturation

As shown in Figure 3, it is also possible to discriminate between complementary and 1-mismatch DNA during denaturation at high frequency (1 MHz). The response time was only 5 minutes.

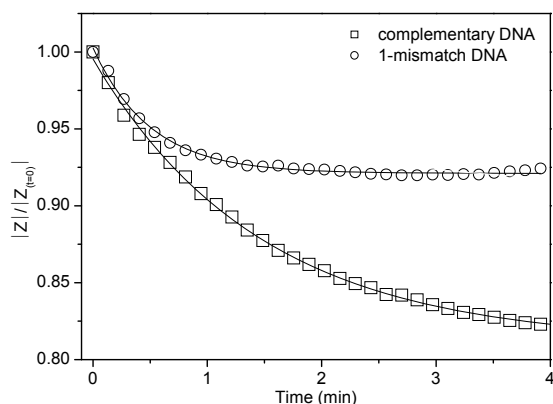


Figure 3: Real-time impedance curves during denaturation of a perfect dsDNA duplex (open squares) and a dsDNA duplex containing a 1-base mismatch (open circles) at 1 MHz.

During the formation of a new equilibrium upon addition of 0.1 M NaOH, the ssDNA molecules and their associated counter-ions leave the double-layer, and enter the solution, resulting in a decrease in R_s . However, as seen in Figure 3, perfect DNA duplexes are typically reflected by a slower impedance decrease kinetic as compared to duplexes with a single nucleotide polymorphism (SNP). This SNP sensitivity is clinically relevant since numerous genetic illnesses are caused by single point mutations. Since complementary duplexes are stable molecules, they have a rather high melting temperature, reflected in a slow impedance decrease rate. SNP-duplexes are much less stable than complementary duplexes, and hence they have a lower melting temperature. This is reflected in a faster impedance decrease rate [6].

This exact principle of SNP differentiation based on different melting temperatures is also the basis of denaturing gradient gel electrophoresis (DGGE) used for SNP identification, but it is the first time that this is reported with an electronic technique. Like is possible with DGGE, EIS could also enable mutation identification, since different types of mutations will also yield duplexes with different melting temperatures.

3.2 Immunosensor

3.2.1 Specificity

CRP-recognition specifically and reproducibly caused an increase in impedance at low frequencies (~ 100 Hz) in real-time within 30 minutes, as compared to treatment with plasminogen. This is demonstrated in Figure 4.

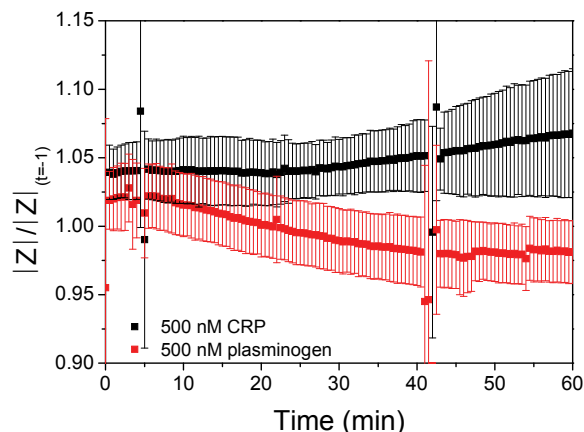


Figure 4: Specificity experiments of the CRP-directed immunosensor with an averaging of real-time impedance spectra taken at 100 Hz during 500 nM CRP addition (black squares) and 500 nM plasminogen addition (red squares).

In order to get more insight in the physical meaning of the impedance variations, the impedance spectra were also analyzed using an equivalent circuit model (Figure 5).

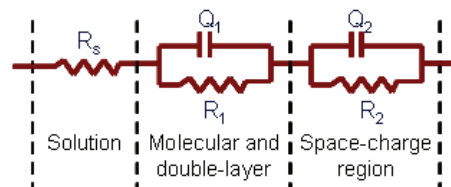


Figure 5: The electrical circuit model used for fitting the impedance data.

It differs slightly from the one used for the DNA-sensor results: (a) the solution resistance R_s , between the Au electrode and the NCD surface, (b) a resistance R_{Q_1} and a constant phase element Q_1 in parallel, corresponding to the molecular layer and its associated double-layer, and (c) a resistance R_{Q_2} and a constant phase element Q_2 in parallel, corresponding to the space-charge region in the NCD. Table 2 shows that the increase of the impedance at low frequencies during CRP treatment corresponds with a significant decrease of the Q_1 value. This was consistently observed, and indicates a smaller capacitance for the molecular layer after CRP recognition at the surface. The additional layer of CRP antigens on top of the anti-CRP antibodies increases the thickness of the molecular layer and changes its dielectric properties, decreasing its capacitance, and thus increasing the impedance.

Element	CRP		Plasminogen	
	Start	End	Start	End
R_s (Ω)	$69.7 \pm 1.3^*$	66.2 ± 0.8	74.1 ± 1.9	81 ± 4
Q_1 ($\mu\text{S}\cdot\text{s}^n$)	0.48 ± 0.05	0.279 ± 0.015	1.3 ± 0.3	1.7 ± 0.7
n	0.77 ± 0.02	0.78 ± 0.01	0.71 ± 0.03	0.69 ± 0.06
R_1 (Ω)	Undetermined			
Q_2 ($\text{nS}\cdot\text{s}^n$)	12.1 ± 0.9	13.3 ± 0.7	21.2 ± 1.9	6.2 ± 0.9
n	0.96 ± 0.01	0.95 ± 0.01	0.89 ± 0.01	0.96 ± 0.01
R_2 ($\text{k}\Omega$)	1.31 ± 0.04	1.28 ± 0.04	7.8 ± 0.4	7.8 ± 0.3

Table 2: Results of fitting the impedance spectra at the start and at the end of CRP and plasminogen.

3.2.2 Sensitivity

As depicted in Figure 6, a clear effect on the impedance is also reproducibly observed in real-time when exposing the anti-CRP-modified NCD samples to different concentrations of CRP. The final CRP concentrations in the wells corresponded to 100 nM, 10 nM and 0 nM. The impedance at 100 Hz changes in a concentration-dependent manner. The lowest concentration of CRP used in our experiments (10 nM) was still clearly distinguishable from the reference channel treated with buffer within 20 minutes.

This indicates the possibility that our prototype immunosensor for CRP can reach a sensitivity within the clinically relevant concentration ranges, important to discriminate between healthy controls (8 – 10 nM) and patients at risk for CVD (>10 nM) [5].

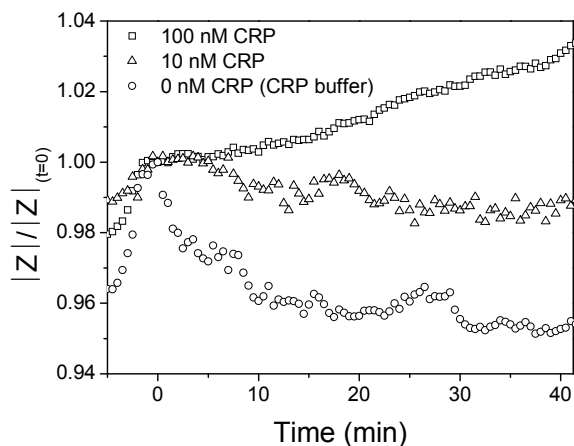


Figure 6: Sensitivity experiments of the CRP-directed immunosensor with real-time impedance spectra at 100 Hz of different concentrations of CRP.

4 CONCLUSIONS

Concerning the development of a prototype of a label-free, real-time electronic DNA-sensor, it was possible to discriminate between complementary and 1-mismatch target DNA during hybridization, in the intermediate frequency region (~1 kHz) in the first 10 minutes after

target DNA addition, but importantly, also during denaturation, at the highest frequency (1 MHz) within the first 5 minutes. The latter could possibly allow SNP-identification. Experiments to optimize this mutation identification are currently being executed.

Also, the potential of EIS for the development of a label-free, real-time electronic immunosensor is demonstrated. A specific discrimination between CRP and plasminogen was obtained in real-time at low frequencies (100 Hz). We also obtained a clinically relevant sensitivity of 10 nM. This specificity and sensitivity will need to be obtained in serum samples as well. These experiments are currently being performed.

REFERENCES

- [1] Yang, W., Auciello, O., Butler, J.E., Cai, W., Carlisle, J.A., Gerbi, J.E., Gruen, D.M., Knickerbocker, T., Lasseter, T.L., Russell, J.N., Jr., Smith, L.M., Hamers, R.J., 2002. *Nat.Mater.* 1, 253-257.
- [2] Field, J.E., 1987. *Inst.Phys.Conf.Ser.* 75, 181-205.
- [3] Christiaens, P., Vermeeren, V., Wenmackers, S., Daenen, M., Haenen, K., Nesladek, M., vandeVen, M., Ameloot, M., Michiels, L., Wagner, P., 2006. *Biosens.Bioelectron.* 22, 170-177.
- [4] Vermeeren, V., Wenmackers, S., Daenen, M., Haenen, K., Williams, O.A., Ameloot, M., Vande, V.M., Wagner, P., Michiels, L., 2008. *Langmuir.* 24, 9125-9134.
- [5] Ridker, P.M., Cushman, M., Stampfer, M.J., Tracy, R.P., Hennekens, C.H., 1997. *N.Engl.J.Med.* 336, 973-979.
- [6] Vermeeren, V., Bijnens, N., Wenmackers, S., Daenen, M., Haenen, K., Williams, O.A., Ameloot, M., vandeVen, M., Wagner, P., Michiels, L., 2007. *Langmuir.* 23, 13193-13202.
- [7] Bijnens, N., Vermeeren, V., Daenen, M., Grieten, L., Haenen, K., Wenmackers, S., Williams, O.A., Ameloot, M., VandeVen M., Michiels, L., Wagner, P., 2009. *Phys.Stat.Sol.(a).* 206, 520-526.